



ELSEVIER

Available online at [www.sciencedirect.com](http://www.sciencedirect.com)

ScienceDirect

journal homepage: [www.elsevier.com/locate/he](http://www.elsevier.com/locate/he)

# The influence of the hydrogenation degree on selected properties of graphane as a material for reversible H<sub>2</sub> storage

Ł. Kaczmarek, T. Warga<sup>\*</sup>, P. Zawadzki, M. Makowicz, B. Bucholc, P. Kula

Institute of Materials Science and Engineering, Lodz University of Technology, Stefanowskiego 1/15 St., 90-924 Lodz, Poland

## HIGHLIGHTS

- Changes in graphane related to the amount of adsorbed hydrogen are investigated.
- Transition between graphane and graphene is examined using modelling software.
- Possible application of graphane in energy storage industry is explained.
- One-sided and completely two-sided hydrogenation of graphane is considered.

## ARTICLE INFO

### Article history:

Received 9 October 2018

Received in revised form

27 May 2019

Accepted 2 June 2019

Available online 7 August 2019

### Keywords:

Graphene

Hydrogen

Hydrogen storage

Graphane

Molecular simulation

## ABSTRACT

This article discusses the effect of hydrogenation of graphane (one-sided and two-side hydrogenation) in relation to the change in the physicochemical properties of graphane as a material capable of reversible H<sub>2</sub> storage. Therefore, the change of the system's energy was determined, differences in HOMO-LUMO molecular levels and the distribution of electrostatic potential as a function of its hydrogenation were simulated. At the same time, the mechanism of graphane reduction to graphene was discussed as a result of interaction with steam from the air. It has been shown that along with the increase in the degree of hydrogenation, the graphane changes its electrostatic potential from negative to positive, simultaneously pushing the negative charge to the edge of the graphane flake. This fact may have an impact on its further chemical reactions, which may significantly limit the sorption properties of graphane. Areas rich in negative charge will prefer chemical reactions with molecules of electrophilic properties, while positive areas with molecules of nucleophilic properties. This determines the elimination of the storage environment of graphane structures used as reversible sources of chemical bonding of hydrogen in order to increase their lifetime as well as sorption capacity.

© 2019 Hydrogen Energy Publications LLC. Published by Elsevier Ltd. All rights reserved.

## Introduction

Currently, intensive work is conducted regarding the development of materials capable of reversible hydrogen storage as

alternative sources of energy. The main areas of application of hydrogen as a fuel are the automotive, aviation and armaments industries, especially in drone propulsion systems. Currently, four methods of hydrogen storage are known and used: in the liquid state [1–3], in the gas state under high pressure [2–5], cryo-adsorption technique [2,6] and storage in metal hydrides [7,8]. However, the most prospective method is

<sup>\*</sup> Corresponding author.

E-mail address: [tomasz.warga@p.lodz.pl](mailto:tomasz.warga@p.lodz.pl) (T. Warga).

<https://doi.org/10.1016/j.ijhydene.2019.06.007>

0360-3199/© 2019 Hydrogen Energy Publications LLC. Published by Elsevier Ltd. All rights reserved.

the storage of hydrogen on carbon structures. The advantages of this type of structures are: (1) high value of kinetics of sorption and desorption processes, (2) low mass compared to current industrial solutions for hydrogen storage and, what is also very important (3) its high chemical and physical stability, (4) no toxicity, (5) limited flammability and explosiveness.

The carbon structures were examined, among others, by teams of prof. Chenga and Khoa Nguyen, including mono- [10,11] and multi-walled [12] nanotubes, fullerenes [13] as well as broadly developing graphene [14]. While carbon systems in the form of nanotubes and fullerenes do not currently allow storage of enough hydrogen to be commercially viable (this limit is 6% by mass [9]), graphene properties allow exceeding this value. This is due to the possibility of its double-side chemical interaction with hydrogen atoms, which significantly shifts the theoretical value of the potential amount of hydrogen storage up to 15%.

According to the literature, however, these studies have not been systematized. Changes in charge distribution on the surface of graphene have not been considered in terms of the ability to chemisorb any subsequent hydrogen atoms. In addition, there is no information on the potential instability of graphane (hydrogenated graphene) and the possibility of its uncontrolled reduction to graphene. Therefore, within this article, the influence of the degree of hydrogenation on the physicochemical properties of graphane and the resulting behavior under natural conditions will be determined.

## Research

First, using the SCIGRESS v.FJ 2.7 program, a graphene structure consisting of 136 carbon atoms was created as a model system of atoms, with 46 hydrogen atoms which saturate bonds with carbon at the edge of the analyzed graphene flake. The system created in this way was optimized in order to achieve the energy minimum. After the optimization of the analyzed graphene structure, the length of C–C bonds is 1.42 Å, while the C–C–C torsion angle is 120°. For such obtained model, computing simulations were carried out using the molecular mechanics.

Next, modelling of molecular systems was performed in which the change in the dihedral angle, bending stresses and

van der Waals forces were analyzed as a function of the change in the number of created C–H bonds at  $sp^2$  hybridization.

In order to determine the chemical stability of hydrogenated graphene systems, the graphene structure prepared in this way was firstly analyzed to determine the Highest Occupied Molecular Orbital (HOMO) and the Lowest Unoccupied Molecular Orbital (LUMO), as well as calculating the thermal energy of the created systems. Then this system was subjected to the hydrogenation process in two variants, forming respectively 2, 4, 8, 16, 32, 48, 64, 80, 96 chemical bonds with carbon atoms of graphene, which corresponded to: 1.5; 2.9; 5.9; 11.8; 23.5; 35.3; 47.1; 58.8 and 70.6% at. hydrogenation of graphene. The first variant of the molecular calculations considered double-side hydrogenation of graphene, while in the second variant, all hydrogen atoms were chemically bound on one side of graphene (Table 1).

During the hydrogenation analysis it was assumed that the hydrogen bound to carbon at the edges of the graphene flake will not be counted in the context of the H/C contribution. For such structures, the change in the HOMO-LUMO energy gap and the heat of structure formation as a function of the increase in the atomic hydrogen share in the chemical reaction with the  $sp^2$  hybridization catalyst were determined.

Based on the analysis of HOMO-LUMO energy gap, one can infer about the chemical stability of the studied systems [15]. In addition, according to Ref. [16], the value of HOMO-LUMO energy gap determines the nature of the material being analyzed (up to 0.3 eV: conductors, 0.3 ÷ 5 eV: semiconductors, over 5 eV: insulators). HOMO and LUMO molecular orbitals for the graphene layer saturated with hydrogen only on the edges are shown in Fig. 1 - structure marked  $G_{0H_2}$ . In Tables 2 and 3, the HOMO and LUMO energies were compared, as well as the HOMO-LUMO energy gap with chemically hydrogenated graphene structures considering their heat of formation for one- and double-sided hydrogenated graphene respectively (see Table 4).

The visible surface polarization of a hydrogenation graphene may translate into a increase of a driving force of chemical reactions, thus decreasing its activation energy. Eventually, the paring of valence electrons will improve the sorption properties of graphene. On the other hand, the phenomenon may influence the sorption degree of hydrogen

**Table 1 – List of analyzed graphene samples depending on the degree of its hydrogenation and the type of structure formed: one-sided or double-sided hydrogenated graphene.**

One-side hydrogenation			Double-side hydrogenation		
Sample	Amount of bonds created through C $sp^2$ +H <sub>2</sub> reaction	Degree of hydrogenation, %	Sample	Amount of bonds created through C $sp^2$ +H <sub>2</sub> reaction	Degree of hydrogenation, %
G <sub>0H<sub>2</sub></sub>	0	0	G <sub>0H<sub>2</sub></sub>	0	0
G <sub>1H<sub>2</sub></sub> 1S	2	1,5	G <sub>1H<sub>2</sub></sub> 2S	2	1,5
G <sub>2H<sub>2</sub></sub> 1S	4	2,9	G <sub>2H<sub>2</sub></sub> 2S	4	2,9
G <sub>4H<sub>2</sub></sub> 1S	8	5,9	G <sub>4H<sub>2</sub></sub> 2S	8	5,9
G <sub>8H<sub>2</sub></sub> 1S	16	11,8	G <sub>8H<sub>2</sub></sub> 2S	16	11,8
G <sub>16H<sub>2</sub></sub> 1S	32	23,5	G <sub>16H<sub>2</sub></sub> 2S	32	23,5
G <sub>24H<sub>2</sub></sub> 1S	48	35,3	G <sub>24H<sub>2</sub></sub> 2S	48	35,3
G <sub>32H<sub>2</sub></sub> 1S	64	47,1	G <sub>32H<sub>2</sub></sub> 2S	64	47,1
G <sub>40H<sub>2</sub></sub> 1S	No possibility to conduct analysis due to the high degree of structural deformation		G <sub>40H<sub>2</sub></sub> 2S	80	58,8
G <sub>48H<sub>2</sub></sub> 1S			G <sub>48H<sub>2</sub></sub> 2S	96	70,6

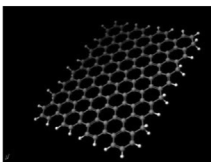
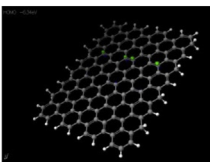
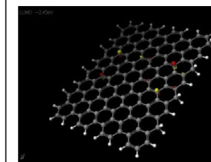
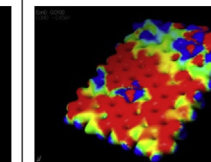
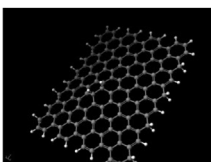
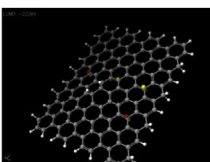
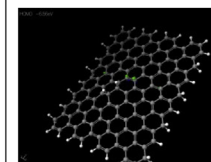
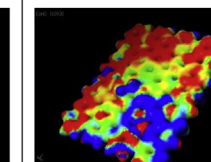
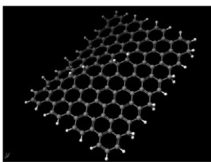
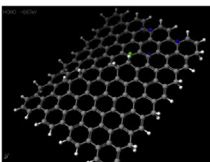
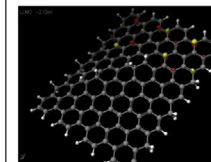
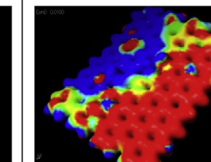
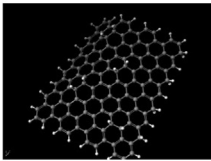
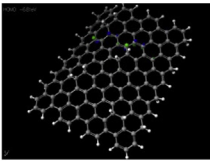
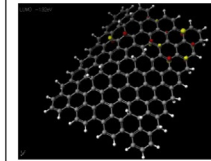
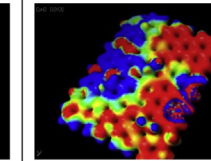
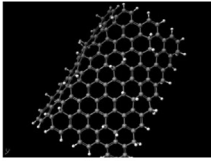
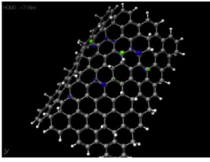
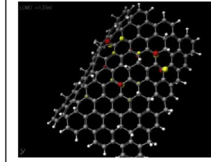
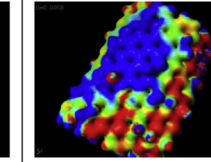
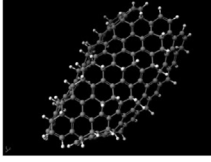
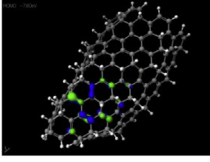
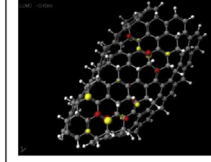
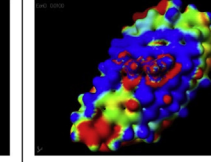
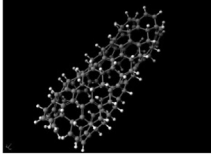

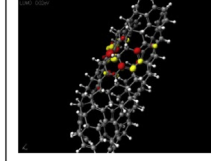
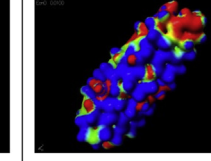
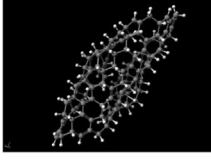
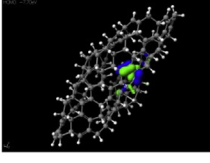
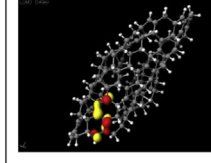
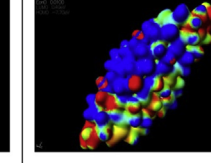
Sample	Structure	HOMO	LUMO	Electrostatic potential
G <sub>0H2</sub>				
G <sub>1H21S</sub>				
G <sub>2H21S</sub>				
G <sub>4H21S</sub>				
G <sub>8H21S</sub>				
G <sub>16H21S</sub>				
G <sub>24H21S</sub>				
G <sub>32H21S</sub>				

Fig. 1 – Structures of one-side hydrogenated forms of graphene along with the distribution of HOMO-LUMO molecular orbitals and electrostatic potential maps (electrostatic potential mapping from the charge density matrix).

**Table 2 – Energy of HOMO, LUMO, HOMO-LUMO gap and heat of creation of chemically one-side hydrogenated graphene structures.**

Structure	HOMO [eV]	LUMO [eV]	HOMO-LUMO energy gap [eV]	Heat of creation [kcal/mol]
G <sub>0</sub> H <sub>2</sub>				
G <sub>1</sub> H <sub>2</sub> 1S	-6,56	-2,23	4,33	423
G <sub>2</sub> H <sub>2</sub> 1S	-6,67	-2,13	4,54	440
G <sub>4</sub> H <sub>2</sub> 1S	-6,81	-1,92	4,89	466
G <sub>8</sub> H <sub>2</sub> 1S	-7,18	-1,37	5,81	511
G <sub>16</sub> H <sub>2</sub> 1S	-7,60	-0,40	7,20	539
G <sub>24</sub> H <sub>2</sub> 1S	-7,54	0,02	7,56	535
G <sub>32</sub> H <sub>2</sub> 1S	-7,70	0,49	8,19	649
G <sub>40</sub> H <sub>2</sub> 1S	No possibility to conduct analysis due to the high degree of structural deformation			
G <sub>48</sub> H <sub>2</sub> 1S				

**Table 3 – Energy of HOMO, LUMO, HOMO-LUMO gap and heat of creation of chemically double-side hydrogenated graphene structures.**

Structure	HOMO [eV]	LUMO [eV]	HOMO-LUMO energy gap [eV]	Heat of creation [kcal/mol]
G <sub>0</sub> H <sub>2</sub>	-6,34	-2,45	3,89	401
G <sub>1</sub> H <sub>2</sub> 2S	-6,56	-2,24	4,32	415
G <sub>2</sub> H <sub>2</sub> 2S	-6,66	-2,17	4,49	425
G <sub>4</sub> H <sub>2</sub> 2S	-6,81	-2	4,81	435
G <sub>8</sub> H <sub>2</sub> 2S	-7,2	-1,55	5,65	462
G <sub>16</sub> H <sub>2</sub> 2S	-7,78	-0,68	7,1	486
G <sub>24</sub> H <sub>2</sub> 2S	-7,82	-0,35	7,47	415
G <sub>32</sub> H <sub>2</sub> 2S	-8,15	0,12	8,27	360
G <sub>40</sub> H <sub>2</sub> 2S	-8,33	0,59	8,92	277
G <sub>48</sub> H <sub>2</sub> 2S	-8,46	0,69	9,15	234

molecules, especially with an increased degree of graphene defects. In the area of structural defects, a negative charge will also gather, which surprisingly will form a driving force for the H\* bond. Of course, an increase in the defects' summary area theoretically decreases the amount of carbon atoms capable of forming chemical bonds with hydrogen.

Due to that, an increase in amount of defects with beneficial distribution of charge on the graphene surface negatively affects the hydrogen sorption properties. However, an increase of hydrogenation degree with a simultaneous push of negative charge to the edge of the structure will also change a type of possible chemical reactions to occur with the graphene (ex. with water vapor), what has been described above.

Based on the HOMO-LUMO energy gap analysis [15], it can be concluded that with increase of hydrogenation the gap size increases as well, which may indicate thermodynamic stability of the analyzed chemical structure (see Fig. 5). However, as explained further below, the thermodynamic stability improves after crossing a certain degree of graphene hydrogenation (Fig. 6). Moreover, a tendency to change the nature of the analyzed material from semiconductor to typical properties of an insulators can also be observed and is the effect of bonding valence electrons which form a delocalized bond during the reaction with atomic hydrogen.

Moreover, HOMO-LUMO energies determine the ability of a molecule to donate or receive electrons. This fact is especially important, since in case of using graphene in hydrogen storage applications, every change its hydrogenation degree influences its reactivity in relation to compounds with donor or acceptor properties. Because of that, any analysis regarding the graphene hydrogenation must be supplemented with calculations of any potential reactions between graphene and chemical compounds present in the surrounding environment, even in trace amounts. This will help determine the environmental parameters that must be taken into account during development stage for a hydrogen storage bed based on graphene. It is crucial to determine the oxidizing potential, which translates to the type of a compound the graphene will react with at different degree of its hydrogenation. According to the research team prof. H.Y [17] and Hong Yan Yue [18], the oxidation potential increases with an increase in the HOMO-LUMO energy gap. Analyzing the energy gap values for the graphene flake being studied, it can be stated that this value increases over 2.3 times (3.89 eV for graphene flakes to 9.15 eV for graphene hydrogenated at 70%) compared to non-hydrogenated graphene flakes. A similar relationship is observed for one-side hydrogenated graphite.

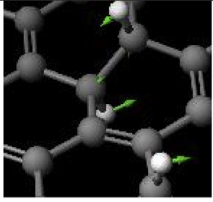
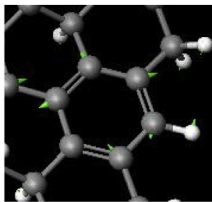
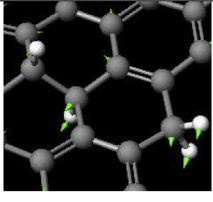
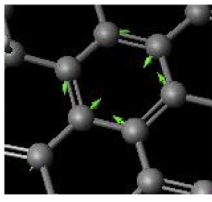
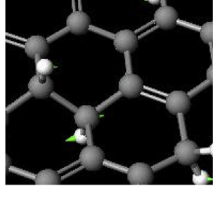
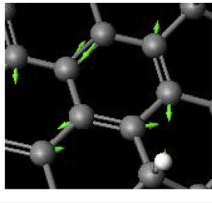
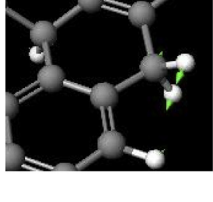
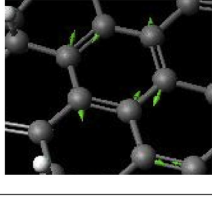
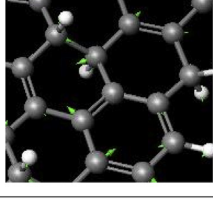
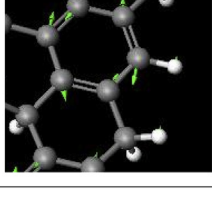
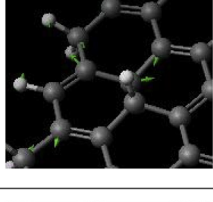
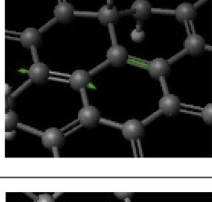
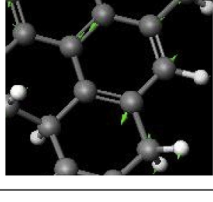
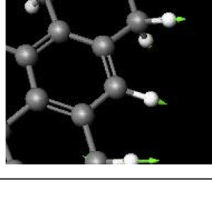
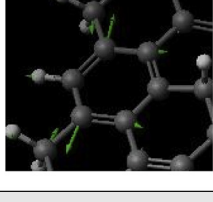
The increase in the oxidation potential of the graphene structure as a function of its oxidation degree is confirmed by the analysis of the distribution of electrostatic potential (Figs. 1 and 2), which is consistent with the research carried out by the team of M Saranya [19]. This correlation is observed both for one- and double-side hydrogenated structures. Red areas in the analysis of the electrostatic potential of the graphene flake with different degrees of hydrogenation mean "negative" zones - "richer" in electrons. On the other hand, the blue color indicates an area poorer in electrons, therefore they take on a "positive" character. Positive areas prefer chemical reactions with molecules with nucleophilic properties. In contrast, areas rich in negative charge will prefer chemical reactions with molecules with electrophilic properties. For this reason, the areas of graphene, in which the sp<sup>2</sup> + H\* hybridization reaction occurs in the C<sub>sp<sup>3</sup></sub>-H binding, are marked as positive zones. In addition, the tendency to push the negative charge on the edges of the flake is clearly marked. A similar relationship was found by X. Duan, K. O'Donnell [20], who analyzed graphene systems doped with sulfur and/or nitrogen.

The occurrence of this phenomenon would explain the reduction of graphene to graphite in the air, which is confirmed by the FTIR spectra of HSMG<sup>®</sup> graphene samples subjected to the hydrogenation process, after which the samples were placed in air atmosphere. After the graphene hydrogenation process, it was observed that contact with air caused a significant drop in its resistance [21]. In this case, ΔR % decreases within 600s from a value close to 340 to 140. The presence of this phenomenon may indicate a reduction of chemically adsorbed atomic hydrogen. The analysis of the FTIR spectra of the hydrogenated samples proved that a new peak appears indicating the appearance of the C-O bond at 1082 cm<sup>-1</sup> (Fig. 3).

Therefore, the following experiment was carried out to determine the effect of the composition of the atmosphere on the dehydrogenation of the graphene layers under analysis. For this purpose, the following atmospheres were



**Table 4 – Different types of molecular vibration and corresponding wavelengths in IR spectra of hydrogenated graphene structures.1**

	- 1141 $\text{cm}^{-1}$ - C-H bond - bending vibration		- 1570 $\text{cm}^{-1}$ - C-C bond - stretching vibration
	- 1148 $\text{cm}^{-1}$ - C-H bond - bending vibration		- 1600 $\text{cm}^{-1}$ - C-C bond - stretching vibration
	- 1218 $\text{cm}^{-1}$ - C-H bond - bending vibration		- 1640 $\text{cm}^{-1}$ - C-C bond - stretching vibration
	- 1290 $\text{cm}^{-1}$ - C-H bond - bending vibration		- 1655 $\text{cm}^{-1}$ - C-C bond - stretching vibration
	- 1350 $\text{cm}^{-1}$ - C-C bond - bending vibration		- 1666 $\text{cm}^{-1}$ - C-C bond - stretching vibration
	- 1410 $\text{cm}^{-1}$ - C-C bond - bending vibration		- 1740 $\text{cm}^{-1}$ - C-C bond - stretching vibration
	- 1440 $\text{cm}^{-1}$ - C-C bond - bending vibration		- 2750-2670 $\text{cm}^{-1}$ - C-H bond - bending vibration
	- 1495 $\text{cm}^{-1}$ - C-C bond - stretching vibration		

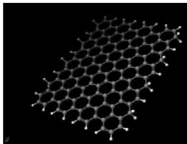
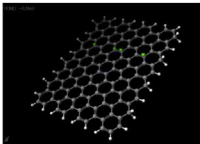
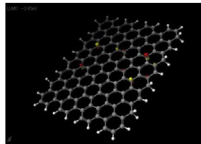
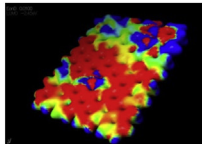
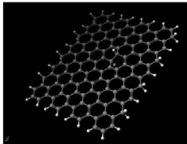
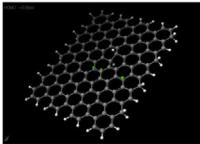
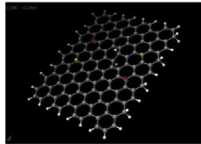
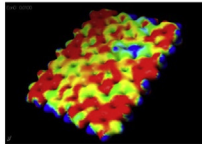
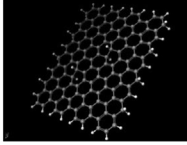
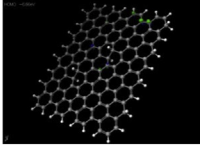
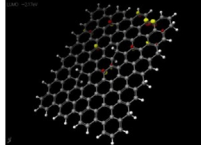
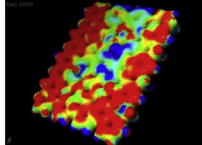
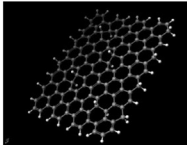
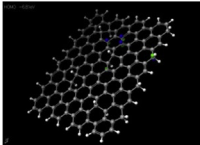
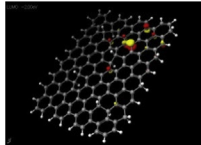
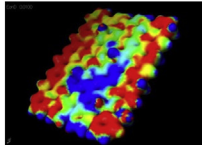
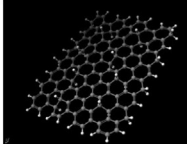
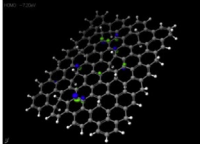
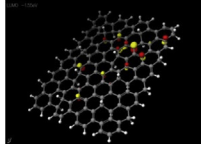
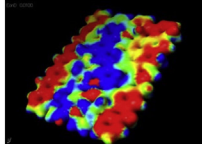
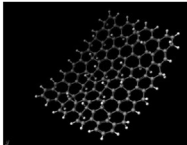
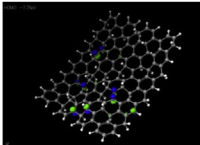
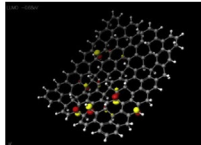
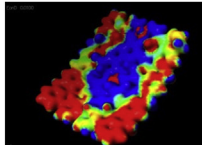
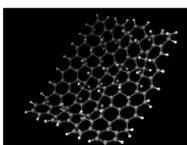
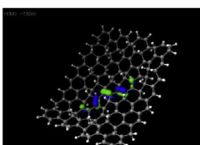
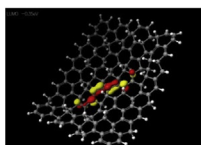
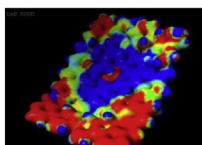
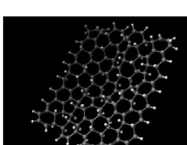
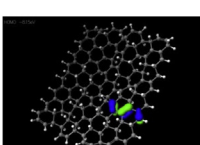
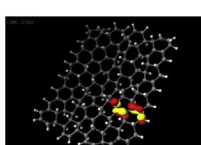
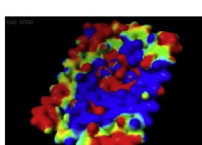
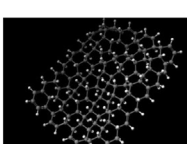
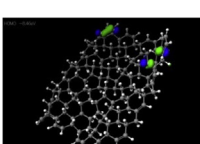
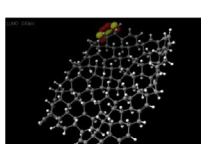
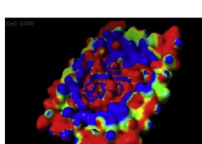
Sample	Structure	HOMO	LUMO	Electrostatic potential
G <sub>0H2</sub>				
G <sub>2H22S</sub>				
G <sub>4H22S</sub>				
G <sub>8H22S</sub>				
G <sub>16H22S</sub>				
G <sub>32H22S</sub>				
G <sub>48H22S</sub>				
G <sub>64H22S</sub>				
G <sub>96H22S</sub>				

Fig. 2 – Structures of double-side hydrogenated forms of graphene along with the distribution of HOMO-LUMO molecular orbitals and electrostatic potential maps (electrostatic potential mapping from the charge density matrix).

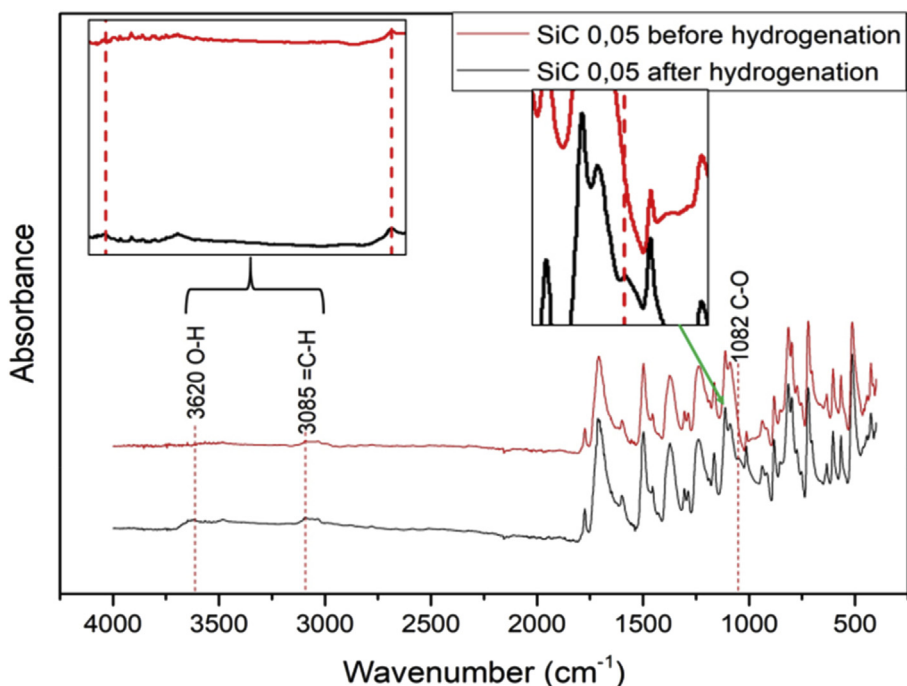


Fig. 3 – Example of IR spectra of HSMG<sup>®</sup> graphene (grown on a forming matrix covered with SiC nanoparticles) before the hydrogenation process (a) and after it with a stage of interaction with steam from the air atmosphere (b).

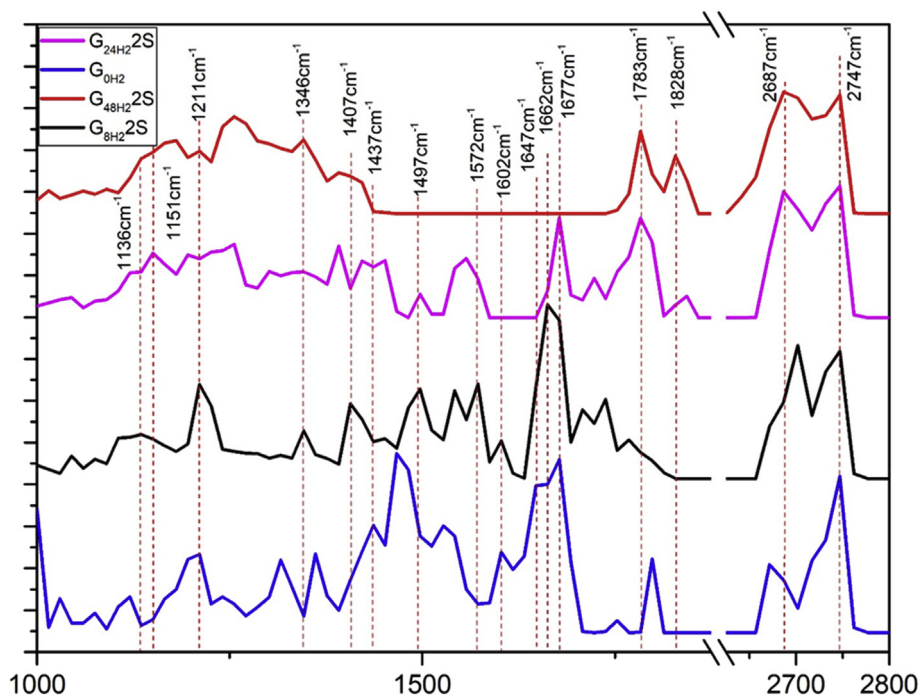


Fig. 4 – Simulated IR spectra for chosen double-side hydrogenated graphene structures.

independently tested, which were introduced in a controlled manner into a vacuum chamber ( $O_2$  or Ar or  $O_2 + H_2O$ ). It has been proven that an intense increase in electron mobility is observed in the  $O_2 + H_2O$  atmosphere. Therefore, it was assumed that the dehydrogenation mechanism is as follows. First of all, condensation of water vapor on the surface of graphene and the formation of hydrogen bonds between the

donor (hydrogen bound to the surface of graphene) and the acceptor (oxygen in the water molecule) is observed. The dissolved oxygen molecule in the environment of the water vapor condensed on the graphene surface dissociates according to the equation (1) forming the  $OH^-$  ions.



In the presence of ions, intensive dehydrogenation of graphene occurs according to reaction (2), as a result of which the reaction is immediate and cyclic due to the formation of water molecules, being the reaction medium, capable of dissolving molecular oxygen and re-generating OH<sup>-</sup> ions.



In order to determine the actual functional groups, present in the structure of graphene flakes - graphane (hydrogenated form), appropriate infrared spectra were simulated using molecular mechanics through the SCIGRESS v.FJ 2.7 software. For this purpose, as a model atomic system, a graphene structure composed of 136 carbon atoms was created, which was subjected to spatial optimization in order to achieve the minimum energy of the system. For the obtained energy-optimized structure, computer simulations were carried out to identify the interaction of infrared radiation with characteristic chemical groups. The following functional groups have been identified corresponding to the characteristic wavelengths.

The spectral analysis proves that with the increase in the degree of hydrogenation of graphene, the intensity of the peak at 1260 cm<sup>-1</sup> and 1360 cm<sup>-1</sup> increases and the intensity of all peaks coming from graphene structure decreases, i.e. in the range 1400–1670 cm<sup>-1</sup> and 1740–2700 cm<sup>-1</sup> (Fig. 4. Table 3).

It is worth noting that the reaction (2) occurs only in case of hydrogen bound with carbon from a graphene structure with sp<sup>2</sup> hybridization, i.e. C<sub>sp<sup>2</sup></sub> + H<sub>2</sub> → C<sub>sp<sup>3</sup></sub>-H. It results from the following fact. On the edge the carbon has sp<sup>3</sup> hybridization, in which the carbon creates two σ bonds with two electrons from sp<sup>2</sup> orbitals of adjacent carbon atoms and one σ with the orbital s of a hydrogen atom. Regarding hydrogenated graphene, the case is sp<sup>3</sup> hybridization of carbon where it forms three σ bonds with three sp<sup>2</sup> electrons of three neighboring carbon atoms and one σ bond with the orbital s of a hydrogen atom. Such a hydrogen bonding system and the formation of

sp<sup>3</sup> carbon hybridization in the graphene structure makes the binding energy equal C<sub>graphene</sub>-H = 35 kcal/mol [22]. However, in case of interaction of hydrogen with defects (edge), a strong tendency to create chemical bonds C<sub>G-edge</sub>-H is observed, in case of which this energy corresponds to the energy of C–H bonds in aromatic compounds and ranges 72–110 kcal/mol.

The increased C–H binding energy on the edges of graphene results from the necessity of saturating the carbon atoms' valence electrons. This causes the reactivity of the system to decrease, with a simultaneous improvement of its thermodynamic stability. Low binding energy of C–H in the graphene structure is related to additional stress inside it. Namely, hybridization change from sp<sup>2</sup> to sp<sup>3</sup> during the creation of C–H bonds causes the graphene to lose its "flatness" and form a local 3D systems. Due to that, contrary to the reactions occurring at the edges of the structure, the thermodynamic stability of the system decreases. The hydrogenated graphene is characterized with a higher energy, so it naturally lowers it by reversing the C<sub>graphene</sub>-H reaction and return to a flat system through the C<sub>graphene</sub>-C<sub>graphene</sub> bonding.

Moreover, due to the generation of relatively high stress in the structure of hydrogenated graphene and associated with it a steric hindrance of C<sub>graphene</sub>-H, the system weakens its binding force. It is possible for it to show bonds in-between the type of chemical binding and physical interaction. It is the result of a possibility of electron exchange between C<sub>graphene</sub>-H bonds and graphene's delocalized bonds.

We presume that the effect of the described phenomena and, as a result, weakening the C<sub>graphene</sub>-H bond dictates its reversible properties. Thanks to that, by properly applying the temperature and pressure of the system, it is possible to achieve the phenomenon of reversible storage of hydrogen. However, any structural defects affect the forming of stable bonds of C<sub>edge</sub>-H, C<sub>defect</sub>-H, which even in the optimal conditions of pressure and temperature, do not undergo the process of reversible binding of hydrogen. Due to that, a crucial parameter of the storing bed is the quality of the graphene

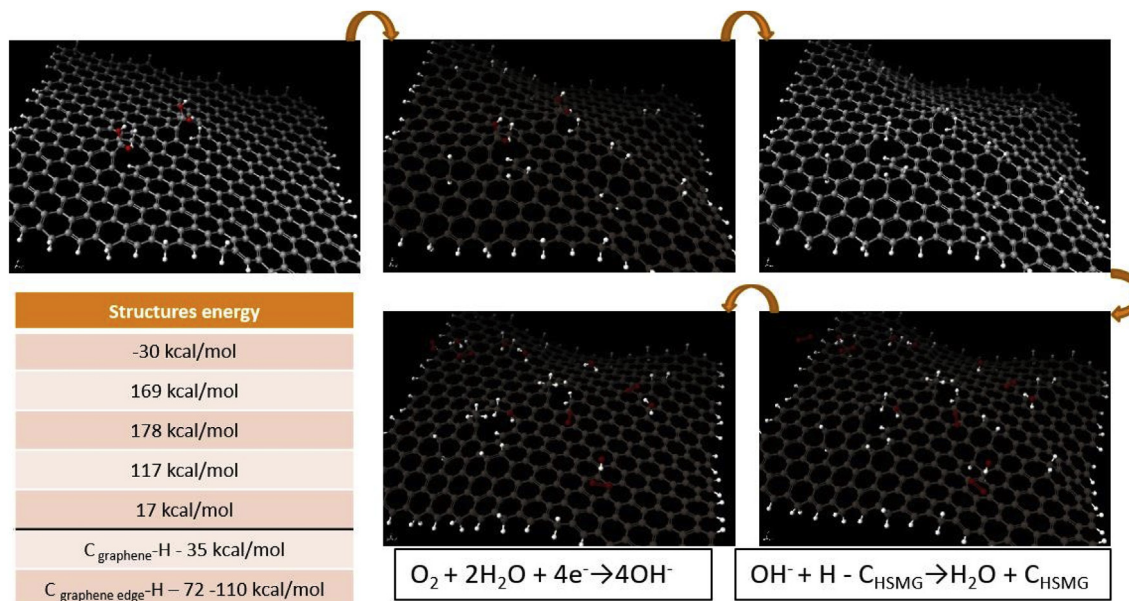


Fig. 5 – Stages of graphene hydrogenation with energy values for each structure.



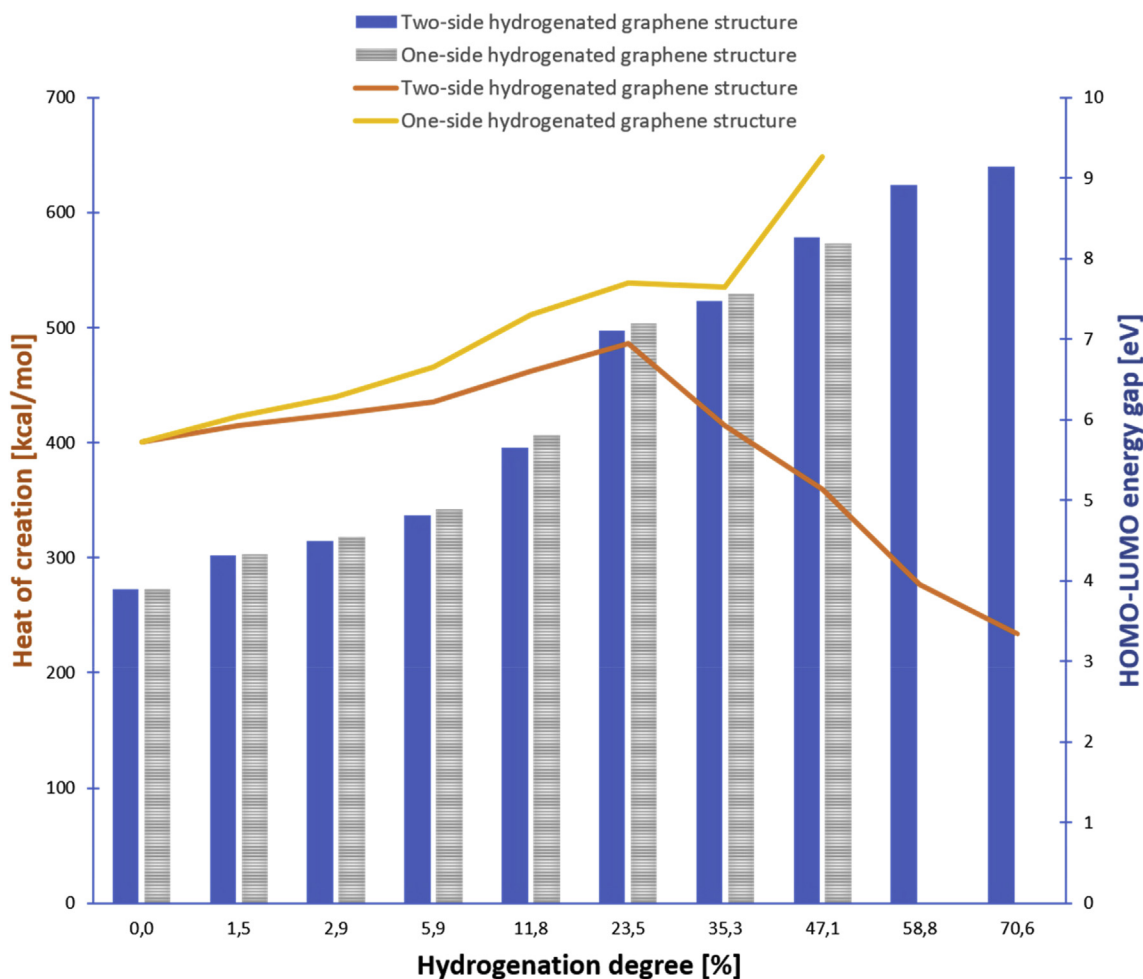


Fig. 6 – Dependence between heat of creation of analyzed structures and their hydrogenation degree as well as the type of structure: one- or double-sided hydrogenated graphene.

that could be estimated by the ratio of  $\frac{C_{sp^3}}{C_{sp^2}}$ , which treats the amount of carbon atoms not taking part in the process of reversible hydrogen storage.

The above phenomena explains why in the cycles of sorption and desorption of hydrogen on graphene sheets, the system virtually returns to the starting point of the resistance value. This insignificant value of  $\Delta R$  is related to the permanent interaction of hydrogen with defects of the graphene structure constituting the holes, the boundaries of polycrystalline graphene [23] and its edges. In this case, the energy of hydrogen-carbon bonds of the graphene system is 35 kcal/mol [17] in contrast to the energy of hydrogen-carbon bonds in aromatic structures being at least twice as high [24–26]. As a consequence, in these conditions hydrogen is not desorbed due to defects.

For this reason, it is important to eliminate even trace amounts of water vapor from tanks intended for the storage of graphene sheets capable of reversibly binding hydrogen. This is crucial in case of eliminating uncontrolled reduction of hydrogenated graphene structures and the formation of water particles in accordance with the above-described mechanism.

At the same time, the heat of creation of the analyzed structures was calculated depending on the degree of their hydrogenation and the type of structure created: one-side or double-side hydrogenated graphene. For both one- and double-side hydrogenated graphene, the heat of formation for all analyzed intermediate systems has a positive value and increases as a function of the degree of hydrogenation. The positive value of the enthalpy of formation indicates that these processes are endothermic.

However, in relation to double-side hydrogenated systems, the increase of this value is observed up to the composition level of chemically bound hydrogen of about 23%. Further delocalization of electrons from atomic orbitals lying perpendicular to the  $\sigma$  plane is energetically beneficial. This effect is achieved after exceeding the hydrogenation degree of 23%. Thermodynamic stabilization of the system to the level of non-hydrogenated graphene energy may result from the fact of reaching the degree of saturation of delocalized bonds. Thus, the occurrence of conjugated multiple bonds is minimized. Then, the structure stabilizes reaching the heat of formation value around 230 kcal/mol for the level of hydrogenation ~70%. For comparison, this value for the simulated,

non-hydrogenated graphene structure is nearly 400 kcal/mol (Fig. 6).

## Conclusion

Based on the analyzes carried out on HOMO-LUMO energy gaps, electrostatic potential distribution as well as FTIR analysis of real and simulated hydrogenated graphene systems, the following correlations were determined:

1. From the point of view of the energy of the system (the possibility of minimizing it), double-side hydrogenation of graphene structures is preferred.
2. With the increase of the graphene hydrogenation degree, one observes:
  - a) The change of its nature from semiconductor (up to 6% at the hydrogenation of graphene) to typical properties as for insulators (difference in HOMO-LUMO energy gap value above 5 eV).
  - b) Increase in the oxidation potential of the graphene structure with simultaneous tendency to push the negative charge on the edges of the analyzed flake.
  - c) An increase in the tendency to reduce in the atmosphere containing water vapor. This is due to increase in the driving force resulting from the change of charge distribution on the graphene surface and a stronger interaction with OH<sup>-</sup> ions. This fact clearly indicates the need to eliminate even trace amounts of residual water vapor in hydrogen storage tanks using graphene structures as a sorbent.

## Acknowledgement

Project co-financed under the 1st competition of the Strategic Research and Development Program “Modern material technologies” - TECHMATSTRATEG.

Agreement No. TECHMATSTRATEG1/347324/12/NCBR/2017.

Project title: “DIAMSEC - ultra-sensitive sensory platform for rapid detection of epidemiological and pandemic threats”.

## REFERENCES

- [1] Habebusch MS, Nguyen CT, Stochl RJ, Hui TY. Development of No-Vent™ liquid hydrogen storage system for space applications. *Cryogenics* 2010;50:541e8.
- [2] Paggiaro R, Benard P, Polifke W. Cryo-adsorptive hydrogen storage on activated carbon. I: thermodynamic analysis of adsorption vessels and comparison with liquid and compressed gas hydrogen storage. *Int J Hydrogen Energy* 2010;35:638e47.
- [3] Zuttel A. Hydrogen storage methods. *Naturwissenschaften* 2004;91:157e72.
- [4] Luxemburg D, Flamant G, Beche E, Sans J-L, Giral J, Goetz V. Hydrogen storage capacity at high pressure of raw and purified single wall carbon nanotubes produced with a solar reactor. *Int J Hydrogen Energy* 2007;32:1016e23.
- [5] Zheng J, Liu X, Xu P, Liu P, Zhao Y, Yang J. Development of high pressure gaseous hydrogen storage technologies. *Int J Hydrogen Energy* 2012;37:1048e57.
- [6] Li J, Wu E, Song J, Xiao F, Geng C. Cryoadsorption of hydrogen on divalent cation- exchanged X-zeolites. *Int J Hydrogen Energy* 2009;34:5458e65.
- [7] Cieslik J, Kula P, Filipek SM. Research on compressor utilizing hydrogel storage materials for application in heat treatment facilities. *J Alloys Compd* 2009;480(2):612e6.
- [8] Cieslik J, Kula P, Sato R. Performance of containers with hydrogen storage alloys for hydrogen compression in heat treatment facilities. *J Alloys Compd* 2011;509(9):3972e7.
- [9] Patchkovskii S, Tse JS, Yurchenko SN, Zhechkov L, Heine T, Seifert G. Graphene nanostructures as tunable storage media for molecular hydrogen. *Proc Natl Acad Sci U S A* 2005;102(30):10439–44.
- [10] Rajaura RS, Srivastava S, Sharma PK, Mathur S, Shrivastava R, Sharma SS, et al. Structural and surface modification of carbon nanotubes for enhanced hydrogen storage density. *Nano Struct Nano Objects* April 2018;14:57–65.
- [11] Cheng H, Yang Q, Liu Ch. Hydrogen storage in carbon nanotubes. *Carbon* August 2001;39(10):1447–54.
- [12] Hou P, Yang Q, Bai S, Xu S, Liu M, Cheng H. Bulk storage capacity of hydrogen in purified multiwalled carbon nanotubes. *J Phys Chem B* 2002;106(5):936–66.
- [13] Durbin DJ, Allan NL, Malardier-Jugroot C. Molecular hydrogen storage in fullerenes – a dispersion-corrected density functional theory study. *Int J Hydrogen Energy* 10 August 2016;41(30):13116–30.
- [14] Gangu KK, Maddila S, Babu S, Mukkamala, B Jonnalagadda S. Characteristics of MOF, MWCNT and graphene containing materials for hydrogen storage: a review. *J Energy Chem* 27 April 2018;30:132–44.
- [15] Seenithuraia S, Pandyan RK, Kumar SV, Mahendran M. Electronic properties of boron and nitrogen doped graphene. *Nano Hybrids* 2013;5:65–83.
- [16] Ouahab L, Yagubskii E. Organic conductors, superconductors and magnets: from synthesis to molecular electronics. Kluwer Academic Publishers Netherlands; 2004. p. 81–98.
- [17] Wang X, Gao D, Li M, Li H, Li C, Wu X, et al. CVD graphene as an electrochemical sensing platform for simultaneous detection of biomolecules. *Sci Rep* 2017;7. Article number: 7044.
- [18] Yue HY, Huang S, Chang J, Heo C, Yao F, Adhikari S, et al. ZnO nanowire arrays on 3D hierarchical graphene foam: biomarker detection of Parkinson's disease. *ACS Nano* 2014;8(2):1639–46.
- [19] Saranya M, Ayyappan S, Nithya R, Sangeetha RK, Gokila A. Molecular structure, NBO and homo-lumo analysis of quercetin on single layer graphene by density functional theory. *Digest J Nanomater Biostruct* January – March 2018;13(1):97–105.
- [20] Duan X, O'Donnell K, Sun H, Wang Y, Wang S. Sulfur and nitrogen co-doped graphene for metal-free catalytic oxidation reactions. *Small* 2015;11:3036–44.
- [21] Kula P, Szymanski W, Kolodziejczyk L, Atraszkiewicz R, Grabarczyk J, Clapa M, et al. High strength metallurgical graphene for hydrogen storage nanocomposites. *Vacuum* 2016;129:79–85.
- [22] Darvish Ganji M, Hosseini-khah SM, Amini-tabar Z. Theoretical insight into hydrogen adsorption onto graphene: a first-principles B3LYP-D3 study. *Phys Chem Chem Phys* 2015;17:2504–11.
- [23] Kula P, Pietrasik R, Dybowski K, Atraszkiewicz R, Szymański W, Kolodziejczyk L, et al. Single and multilayer growth of graphene from the liquid phase. *Appl Mech Mater* 2014;510:8–12.

- 
- [24] van Scheppingen W, Dorrestijn E, Arends I, Mulder P. Carbon–Oxygen bond strength in diphenyl ether and phenyl vinyl Ether: an experimental and computational study. *J Phys Chem A* 1997;101:5404–11.
- [25] Zhu XQ, Li HR, Li Q, Ai T, Lu J-Y, Yang Y, et al. Determination of the C4-H bond dissociation energies of NADH models and their radical cations in Acetonitrile. *Chem. Eur J* 2003;9(4):871–80.
- [26] Laarhoven LJJ, Mulder P, M Wayner DD. Determination of bond dissociation enthalpies in solution by photoacoustic calorimetry. *Acc Chem Res* 1999;32:342–9.